AIAA 2002-3159

Overview of Active Flow Control Actuator Development at NASA Langley Research Center

Norman W. Schaeffler, Timothy E. Hepner, Gregory S. Jones, and Michael A. Kegerise

NASA Langley Research Center, Hampton, VA
United States of America

1st AIAA Flow Control Conference
June 24–26, 2002/St. Louis, Missouri

Overview of Active Flow Control Actuator Development at NASA Langley Research Center

Norman W. Schaeffler*, Timothy E. Hepner†, Gregory S. Jones*, and Michael A. Kegerise*

NASA Langley Research Center, Hampton, VA
United States of America

The paper provides an overview of the actuator development work that is currently underway at NASA Langley Research Center in the context of some of the Active Flow Control research being conducted at NASA Langley. The actuator development effort has provided a focused, centralized location for this work within NASA Langley. The multidisciplinary team approach utilized in this effort has allowed input from multiple disciplines on how various actuator challenges can be addressed and has lead to some unique approaches in actuation.

Introduction

FOR longer than the concepts of a boundary layer and separation have existed in the lexicon of aerodynamics, humanity has sought ways to exercise control over them. In the same paper in which Prandtl[1] introduces the concept of the boundary layer, Prandtl also discusses separation and presents an experimental technique for eliminating it. In the intervening century, the search for more efficient and robust means of control has continued. In the future, we seek not only to suppress transition or separation, but to control its development and evolution. To identify techniques for virtually and dynamically shaping aerodynamic bodies allowing for a tailoring of the aerodynamic force, instant by instant. Realization of these goals for flow control will allow aerodynamic design to move from a compromised limited set of design points to adaptive designs that are capable of efficient operation over a broad spectrum of flight envelopes.

NASA Langley has figured prominently in the last four of the "five eras of flow control" as defined by Gad-el-Hak,[2] having not existed during the "first era". Advances in laminar flow control[3] and the invention of large-eddy breakup devices, riblets, and micro-vortex generators are just a few of the examples given by Gad-el-Hak of technologies developed at NASA Langley. Recent overviews have provided snapshots of the research in active flow control being conducted at the Center.[4–6]

In order to accomplish these new goals for flow control, there must be some type of Active Flow Control (AFC) actuators. Either surface-based actuators, where some appendage of the aerodynamic body interacts with the freestream and/or the boundary layer, or fluidic-based actuators, where the flow is controlled by the removal or the addition of momentum to the freestream. This paper summarizes the development of actuators for AFC currently underway at NASA Langley Research Center. The actuator design methodology is being pursued as a multidisciplinary, cooperative effort, involving experimental fluid mechanics, computational fluid mechanics, electronics and material science. The actuator development effort at NASA Langley seeks not only to identify aerodynamic situations that can be successfully managed by existing classes of flow control actuators, but to also shed some light on the physics of the interaction between the actuator and the flow it is trying to control. Traditionally, the first step in actuator development has been that the actuators themselves have been developed and studied. Then as many applications as possible were found for these newly developed actuators. By studying the physics of the actuator-flow interaction, a coherent picture of how a certain actuator type is able to control its target flow can be developed. This will then allow actuator development to start with a set of target flow-based requirements and then develop an actuator to fulfill these requirements, as opposed to finding an applicable flow once the actuator has been developed. In this paper, we will examine the actuator research and development work that was done to support research in the following flow control areas:

- Noise reduction in cavity flows.

*Research Scientist, Flow Physics and Control Branch, AIAA member.

†U. S. Army Aviation and Missile Command, Aeroflightdynamics Directorate, Joint Research Program Office.

- Unsteady circulation control wing.
- Synthetic Jet characterization for next generation tool development.
- Conformal Synthetic Jets for separation control and drag reduction.

Active Control of Cavity Flows

Cavity flows are characterized by a complex feedback process that leads to self-sustaining oscillations at a discrete set of frequencies. In many cases, these frequencies experience nonlinear interactions and mode switching.[7–9] The source of these tonal frequencies, known as the Rossiter frequencies, is the interaction of the free-shear layer shed at the leading edge of the cavity and the acoustic waves emanating from the organized vortical structures of the shear layer impinging on the trailing edge of the cavity. The organized vortical structures can be seen in Figure 1, which displays a set of phased-locked Schlieren photographs of the flow over a cavity with a length to depth (L/D) ratio of 2.

The developing shear layer structures and the acoustic disturbances reinforce one another resulting in an amplified acoustic field around the cavity. An open weapons bay on an aircraft is one practical example of a cavity flow. Here, sound pressure levels associated

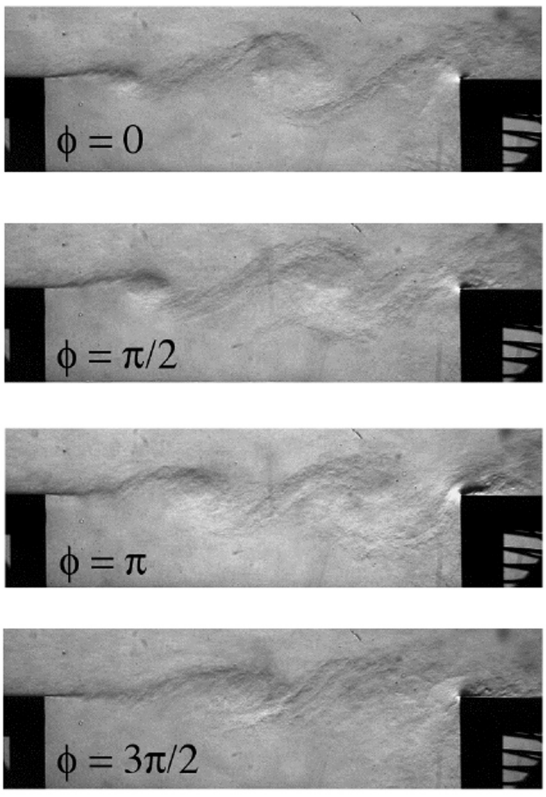

Fig. 1 Phase-Locked Schlieren photographs of the flow over a L/D = 2 Cavity.[8]

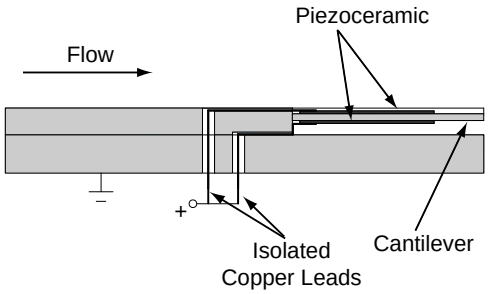

Fig. 2 Schematic of piezoelectric bimorph actuator assembly.

with the flow oscillations are in excess of 170 dB, causing damage to internal stores. It is therefore desired to suppress the cavity oscillations through active flow control.

A central component of an active controller for a cavity flow is the actuator. The main objective of a cavity controller is one of disturbance rejection at the cavity leading edge. To this end, an actuator must have sufficient bandwidth (as large as the maximum Rossiter frequency of interest), must be able to produce disturbances at multiple frequencies, and must have an amplitude response that is large enough to counteract the natural disturbances present in the shear layer. In general, it is difficult to meet all of these requirements simultaneously. Piezoelectric driven flap-type actuators provide a good balance between the conflicting requirements for a control actuator. Piezo flaps can achieve bandwidths in excess of 1 kHz and have recently been shown to produce large streamwise disturbances with micrometer-scale displacements.[10,11]

A schematic of the piezoelectric bimorph actuator used in our cavity control studies is shown in Figure 2. In cooperation with the University of Florida, a structural dynamics model, coupled to an optimization scheme, was developed to calculate the design parameters of the actuator.[10] The actuator consists of an aluminum cantilever beam to which piezoceramic wafers are bonded with a non-conducting epoxy adhesive. The actuator structure and cantilever beam are electrically grounded for safety reasons. Isolated coppers leads (connected in parallel) provide high voltage to the electrodes of the piezoceramics. A fiber-optic sensor embedded beneath the actuator tip provides an *in situ* measure of the output displacement. The measured transfer function of the actuator for wind-off conditions and three flow conditions is shown in Figure 3. The actuator provides the required tip displacement, which is on the order of 6-17 wall units of the incoming turbulent boundary layer.

As seen in Figure 3, the presence of cross-flow over the actuator surface has little influence on the dynamic response. These measurement allay previous concerns that flow over the actuator damps its response and therefore limits the performance of an active con-

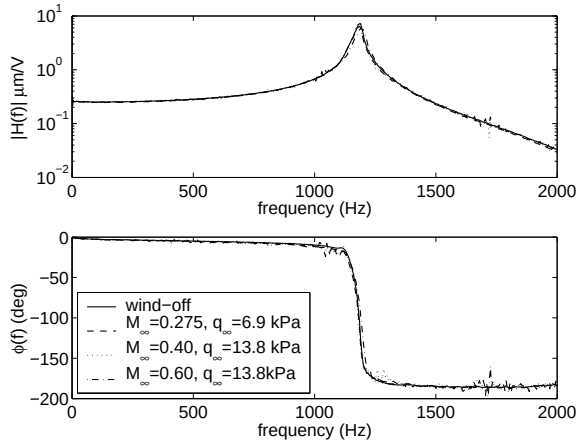

Fig. 3 Frequency response function of the piezoelectric bimorph actuator

troller.[12] A simple gain-delay feedback controller was tested to verify the suitability of the present actuator for multiple tone suppression.[11] Multiple tone reductions of 7 dB were achieved, providing confidence in the actuator for further control studies.

Unsteady Circulation Control Wing

The idea of a circulation control wing, or a wing that is able to tailor its circulation through the use of pneumatic modifications and the Coanda effect, has existed for roughly 65 years. Englar,[13] in his review article, traces the first use of blown jet airfoils back to the 1930's and also to Coanda's original work in 1935. The circulation control wing with a blown Coanda surface at its trailing edge offers the possibility of a high degree of boundary layer control and also for modifications to the global flowfield significant enough to generate 2-D lift coefficients as high as 20 without moving parts.[13] A significant amount of work has been done in the the area of circulation control, especially in the last 40 years, across the spectrum of aerodynamic problems from micro-air vehicles to tractor trailers.[13]

All of this attention is warranted because a circulation control wing would offer significant advantages, specifically to general aviation and to the achievement of personal air vehicles. In addition to high 2-D lift coefficients, advantages include the ability to shorten take-off and landing distances, reduce wing areas, reduce part counts and mechanical complexity, and for weight savings would all be of significant advantage in each of these industries. The downside of the use of a such a flow control device is the need for a compressed air supply to create the flow control jets. The "cost" associated with generating this compressed air, either directly by a compressor or by using air bled from the engines, has usually been judged to outweigh the benefits of using such a device. This would not be the case if it could be shown that the same benefits could be achieved using pulsed, or unsteady jets to interact with the Conada surface, producing the same effect with significantly less mass flow. In the project currently being pursued at NASA Langley, such a arrangement is being tested.

In this work, a Coanda surface has been added to the trailing edge of a general aviation airfoil. Tangent to the the upper and lower surface of the Coanda surface, and embedded within the wing, are the actuation jets. A schematic of this model can be seen in Figure 4. Actuation of the upper and lower jets is independent of one another, which allows the use of this device as a pneumatic flap. Blowing of the upper jet will create significant turning of the flow around the trailing edge, resulting in a high-lift configuration, while balancing the two jets produces a streamlining of the trailing edge at cruise. The arrangement of the Coanda surface and the jets can be seen in Figure 5. The color contours in Figure 5 are contours of Mach number and are one result from the extensive amount of CFD analysis done on this model geometry prior to the actual wind tunnel entry. Utilizing the NASA Langley FUN2-D CFD code, the computations were used to refine the model design and the model wind tunnel test matrix prior to the actual wind tunnel tests.[14]

The flow control actuator capable of producing the pulsed jet flow is a high-performance solenoid value. It is also a commercial, off-the-shelf (COTS) item that is now being employed as a flow control actuator. This COTS device is the result of a massive amount of engineering development, optimizing the design to a specific non-flow control application. However, with some modifications, the device also satisfies a number of the requirements for a flow control actuator. The modifications include changes to the drive electronics and the addition of individual diffusers to the actuators. The actuator, and its assembly details, and the diffuser can be seen in Figure 6.

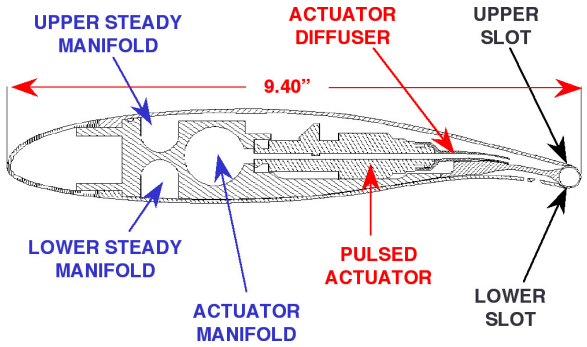

Fig. 4 Schematic of the cross-section of the General Aviation Circulation Control (GACC) model.

The aerodynamic performance benefit and reduced mass flow requirements for pulsed or unsteady circulation control have been suggested by experimental and CFD efforts. NASA Langley has developed a test program to investigate the physics of a Circulation

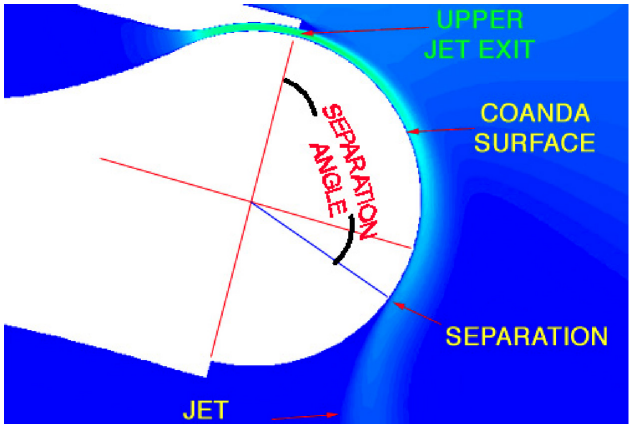

Fig. 5 Nomenclature and CFD Results for the General Aviation Circulation Control (GACC) wing.

a) Photograph of Actuator and Diffuser

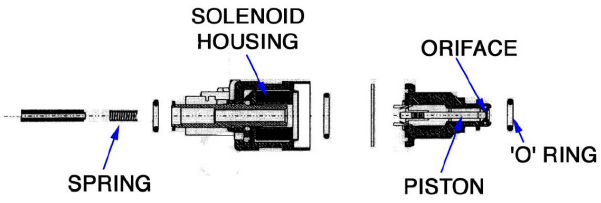

b) Assembly details of the Actuator

Fig. 6 The COTS Pulsed Solenoid Actuator

Controlled Wing (CCW) for general aviation applications as part of the "Active Flow Control" program. This test bed provides a research platform for actuator development that focuses on added mass systems. The General Aviation Circulation Control (GACC) model has the capability of steady and pulsed blowing using 20 actuators placed near the upper surface trailing edge slots. A schematic of this arrangement and a picture of the completed model mounted in the NASA Langley Research Center Basic Aerodynamics Research Tunnel (BART) can be seen in Figure 7.

The COTS actuators provide a square wave type pressure pulse that can be varied in frequency ($5 < \text{Hz} < 200$),duty cycle ($20\% - 100\%$), and velocity magnitude ($0.0 < \text{Mach} < 1.0$). The output of a single actuator as a function of time can be seen in Figure 9. This output was measured one inch downstream of the actuator exit. As can be seen in this figure, the actuator can produce velocities on the order of 825 ft/sec. In application on the model as a flow control device, these actuators are based on added mass and can sustain high velocities for large portions of their duty cycle. Figure 8 shows an example of the surface velocity field one inch downstream of the actuator when installed on the model. To distribute the high velocity pulse train, individual rapid diffusers were developed to maintain uniform flow along the span of the 28-inch slot. These diffusers feed the upper plenum and can be augmented with steady air. Each actuator is independently controlled, creating the ability to generate a unique span-wise loading. The results from this wind tunnel test are discussed in the recent paper by Jones, et. al.[14]

The Synthetic Jet Actuator

The synthetic jet actuator has received a great deal of attention from the research community in the past few years due to its promise as a flow control actuator. The device itself was examined and documented[15] and then the original team applied the technology to control a number of flows.[16,17] Moreover other researchers, including several at NASA Langley,[18] have also documented the basic characteristics of the synthetic jet, refined the design, and applied synthetic jets as a flow control actuator.[19]

Given the role that the synthetic jet has played in recent progress in flow control, it was chosen as the subject of a combined experimental and computational research effort. The end goal of the experimental side of this effort was to provide an unambiguous benchmark dataset for CFD code validation and next generation design tool development. To accomplish this, the flowfield generated by a single synthetic jet issuing into a quiescent environment would be measured by stereo particle image velocimetry (PIV), laser velocimetry (LV), and hot wire anemometry. Also the

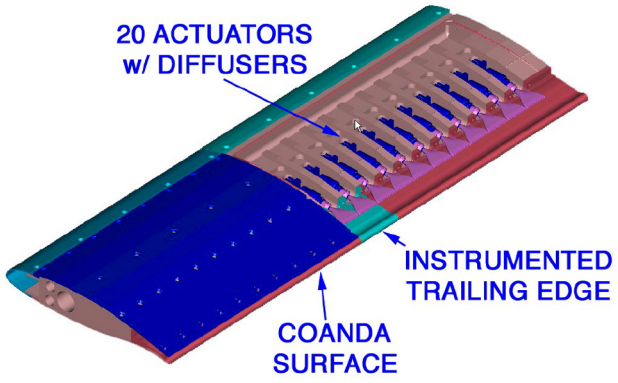

a) Schematic of the wing with panel removed

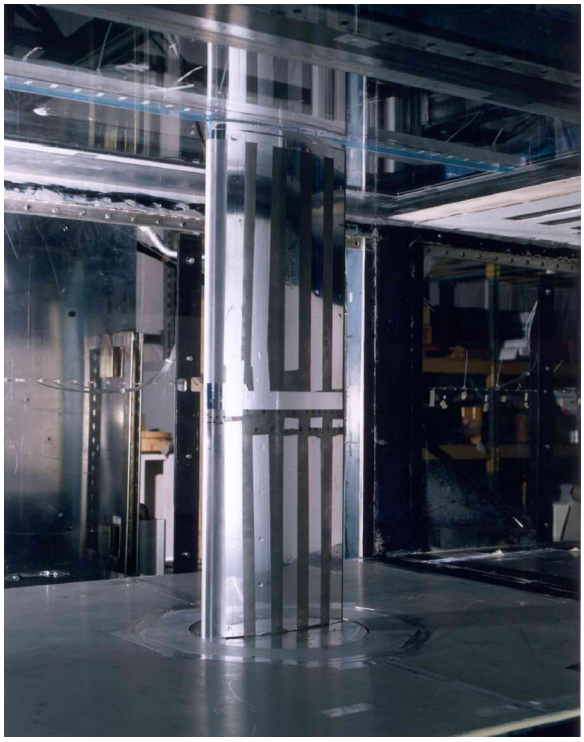

b) Photograph of model installed in the NASA Langley BART

Fig. 7 The General Aviation Circulation Control (GACC) wind tunnel model.

effect of different processing algorithms for the PIV systems and different frequency domain analyzers for the LV systems would be considered. All of these measurements techniques are being brought to bear on this problem in an effort to sort out the experimental uncertainty and allow these measurements to be a direct quality comparison between the computational results and experimental results. By doing so, the state-of-the-art for time-accurate CFD calculations will be advanced.

In another effort to advance the development of the next generation of design tools, NASA Langley is sponsoring, via a grant to University of Florida, research into the theoretical modeling of a synthetic jet actuator. This research effort centers on the use of a lumped element methodology to arrive at an equivalent circuit representation of the synthetic jet. Researchers at NASA Langley are working closely with and supplying experimental data to researchers at the University of Florida to support the development of this design tool.[20]

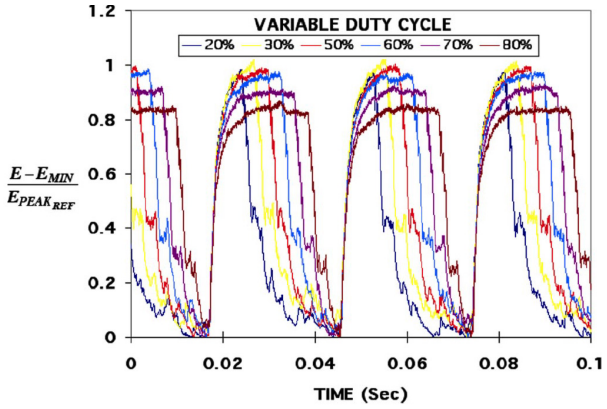

Fig. 8 Normalized Thin Film Time history for pulsed CCW at the slot exit. Frequency: 35 Hz.

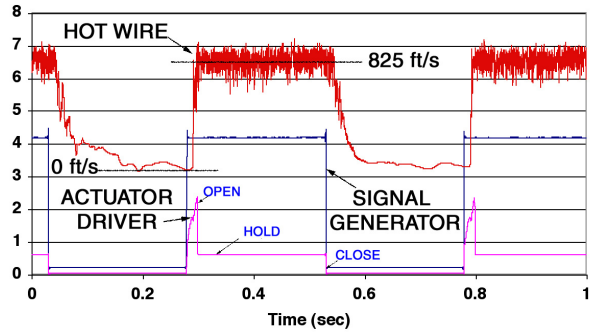

Fig. 9 Velocity, command signal, and actuator drive signal for the COTS actuator as functions of time.

In addition to the interaction of the synthetic jet and a quiescent environment, the dynamics of the interaction of a synthetic jet with a crossflow have also being examined in great detail. By utilizing stereo particle image velocimetry (SPIV), the three components of the velocity field above the actuator were measured and studied. This allows both the instantaneous and phase-averaged interactions between the synthetic jet and a cross flow with a turbulent boundary layer to be examined.

Establishing a CFD Benchmark for the Synthetic Jet

In order to establish a CFD benchmark for the development and refinement of the next-generation of flow control design tools, a standard design of a synthetic jet was agreed upon for both the experimental work and the computations. The details of the design can be seen in Figure 10. Also, it was decided that the

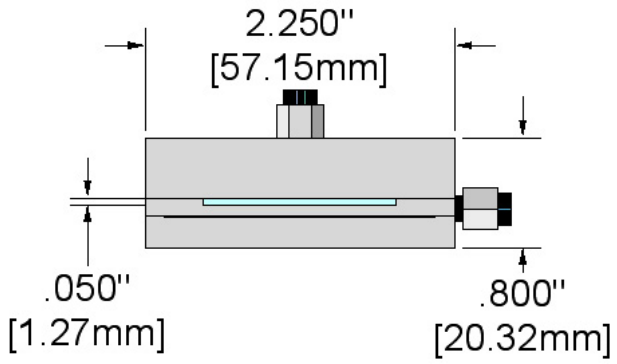

a) Dimensions of the reference actuator

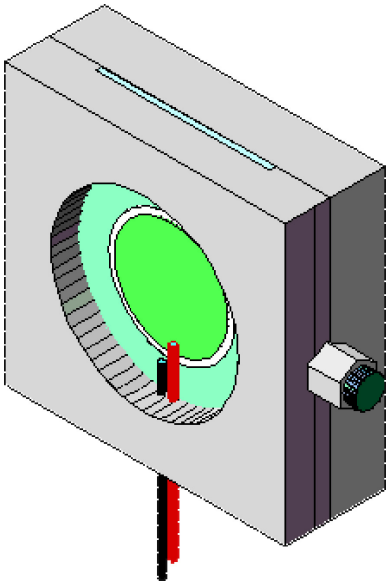

b) 3-D view of actuator with pressure transducer installed

Fig. 10 The CFD Benchmark Reference Synthetic Jet Actuator.

case of the flowfield generated by a single jet issuing into a quiescent environment would be examined first. The adopted design is a synthetic jet with a single diaphragm oriented in plane parallel to the slot axis with a slot width of 1236 microns. For the experimental work, the flowfield has been mapped out in detail by both hot wire anemometry and by Laser Velocimetry. In addition, the jet itself was instrumented in order to be able to record the internal pressure, temperature and diaphragm displacement.

The LV dataset consists of a set of three-dimensional velocity measurements. These measurements made on a plane that was oriented across the slot at its centerline. Three different measurement grids were utilized with spacings of 1000 μm, 250 μm, and 50 μm. The effective sample volume and thus spatial resolution was 100 μm. The synthetic jet was driven by a 450 Hertz amplified sine wave from a function generator. For each velocity measurement, analog-to-digital

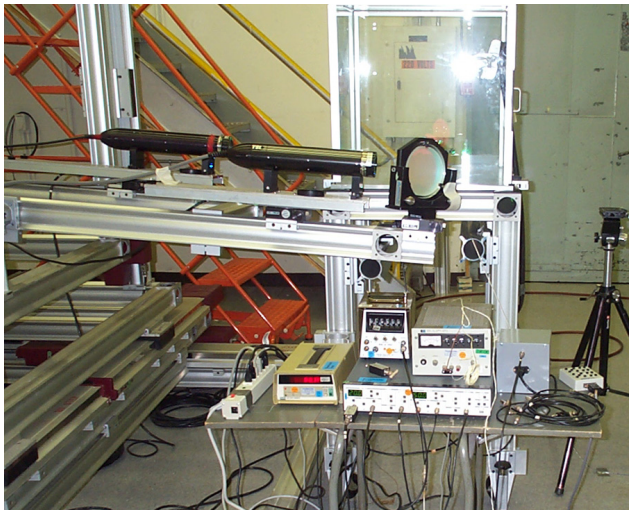

Fig. 11 Part of the Optics Setup for the 3-Component LV System

(A/D) converters measured the signals from the function generator, drive and synch, along with diaphragm displacement and cavity pressure. The temperature in the cavity was measured by a thermocouple and stored along with the data sets from each grid location. The 1000 μm data was averaged in 15-degree increments using the displacement data as the reference. The 250 μm and 50 μm data sets were averaged in 5-degree increments using the displacement data as a reference.

Laser Velocimeter System

The Laser Velocimeter (LV) system was an orthogonal crossed-fringe Fiber optic probe configuration with the receiving optics mounted 90° off-axis. The 514.5, 496.5, and 476.5 nanometer wavelengths from an Argon-Ion laser were used to measure the across the slot (V), vertical (W), and along the slot (U), velocity components respectively. The scattered light from the U, V components was received by the W optics package and the scattered light from the W component was received by the U, V optics package. This setup can be seen in Figure 11. Bragg cells were used to provide directional measurement capability in all three velocity components. Both fiber optics probes used 750-mm focal length lenses, which along with an input beam diameter of 3 to 4mm, generated a sample volume calculated to be approximately 100 μm in diameter and spherical in shape. The fiber optics probes and mirror were mounted on a X95 rail frame and tilted 4.5 degrees down and 3.5 degrees left. The assembly moved as a unit on a traversing system that provided 1 meter of travel, with 10 μm resolution in all three axes.

The synthetic jet was mounted in the floor of a box with a glass top. This glass box was seeded with monodisperse 0.86 μm polystyrene latex micro spheres. The seed particles were suspended in 100-proof alcohol and

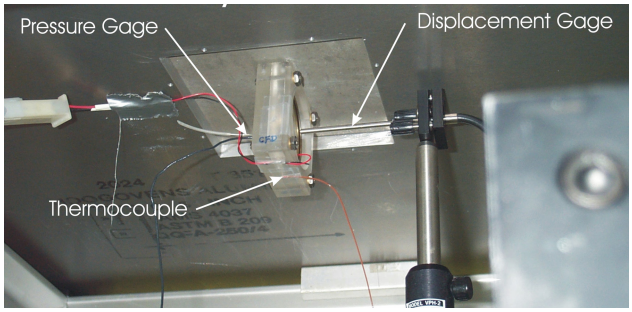

Fig. 12 Instrumented Reference Synthetic Jet. View is from underneath the test section.

atomized by a six-jet atomizer and vented into the box between measurements as necessary. The particles were fabricated at NASA Langley using the technique described by Nichols.[21]

The ability of a particle to track the streamlines in the flow field, and thus the ultimate accuracy of the LV, is related to the size of the particle. Dring and Suo[22] reported theoretical predictions of particle trajectories in swirling flows and concluded that the particle trajectory in a free vortex swirling flow is governed by the Stokes number (S_t) and when the Stokes number is less than 0.01, the particle will follow the circular streamlines of a free vortex. The 0.86 μm particles used in this test, have a density $r_p = 1.04996\ g/cm^3$ and a Stokes number less than 0.01 and will yield a tracking fidelity sufficient to follow the streamlines of the flows at the measurement locations in this test.

To enhance the knowledge about the synthetic jet, a displacement gage was mounted to track the diaphragm's motion and a pressure gage and thermocouple monitored the cavity's pressure and temperature. These pieces of instrumentation can be seen in Figure 12. The output voltages from the drive source (sine wave and synch), displacement gage and pressure transducer were measured with A/D converters synched to the LV system data processor. Logged with every U, V, or W velocity measurement and time stamp was a synched A/D measurement of drive signal; drive synch, pressure, and displacement. The velocity measurements were validated within 5 micro seconds of the end of burst and the A/D's were read from 0 to 20 micro seconds after the velocity signals validation.

The LV data acquisition system software for this test was written in-house using a commercial object-oriented development package enabling the data acquisition software to be run on multiple platforms including Macintosh, IBM PC's or compatibles, and HP RISC workstations. For this series of tests, a PC was utilized. The data processing software was also written in a commercial object-oriented development package. One of the unique capabilities of the processing software is to extract phase lock data. It does this by using the A/D data from the drive and synch signals from the function generator to select data points within a band of degrees, for example from 15 to 20 degrees for each data location. The statistics of the new data ensembles were than calculated.

Once the phase-averaged data has been computed, the resulting dataset is useful not only for direct comparison of the computational results, but also for insight into the characterization of the synthetic jet flowfield. In order to gain some insight into the physics of the development of the synthetic jet flowfield, a visualization scheme was developed that allowed a number of massless particles to be convected through the measured velocity fields. This allows the motion of the particles to be followed as the jet runs through one complete cycle. This visualization scheme was programmed as a network for OpenDX.[23] OpenDX is a open source, general purpose visualization package which is based on the released source code of the IBM Data Explorer software package. Using OpenDX, a set of particles were selected and their displacement recorded as the velocity field changed as a function of time constructing a pathline, i.e. lines are constructed that represent the motion of a single particle during the complete cycle of the jet. The velocity field was interpolated between phases as needed to insure a smooth and accurate particle path. The pathline being constructed is a sectional pathline, meaning that even though all three components of velocity were measured, all of this data still only lies on a single plane. Therefore, the particles are being artificially constrained to remain on that plane and only the in-plane velocity components contribute to the displacement of the particle. Even with this restriction, this technique can yield useful information. Figure 13 illustrates the pathlines for a set of particles released at the beginning of the actuator drive cycle. Here it can be seen that each of the particles are drawn in sequence, starting at the jet edge and progressing to the centerline, into "orbit" around the developing vortex core and then are expelled into the interior of the jet. The particles that are closest to the edge of the jet at the beginning of the cycle are the ones that travel the greatest distance away from the wall by the end of the cycle. The particles that start near the centerline are not able to progress as far away from the wall. A different view of this can be obtained if we consider the position of the individual particles as the velocity field develops in time, as shown in Figure 14. Here we can see how a set of particles placed above the slot at the beginning of the actuator cycle move away from the actuator, develop into and are convected away from the wall by the formed vortex pair and the eventual decay of the vortex pair.

Once the phased-averaged velocity field has been established, it can be averaged again across all the phases to yield the mean velocity field for the synthetic jet. The streamlines for this case are displayed

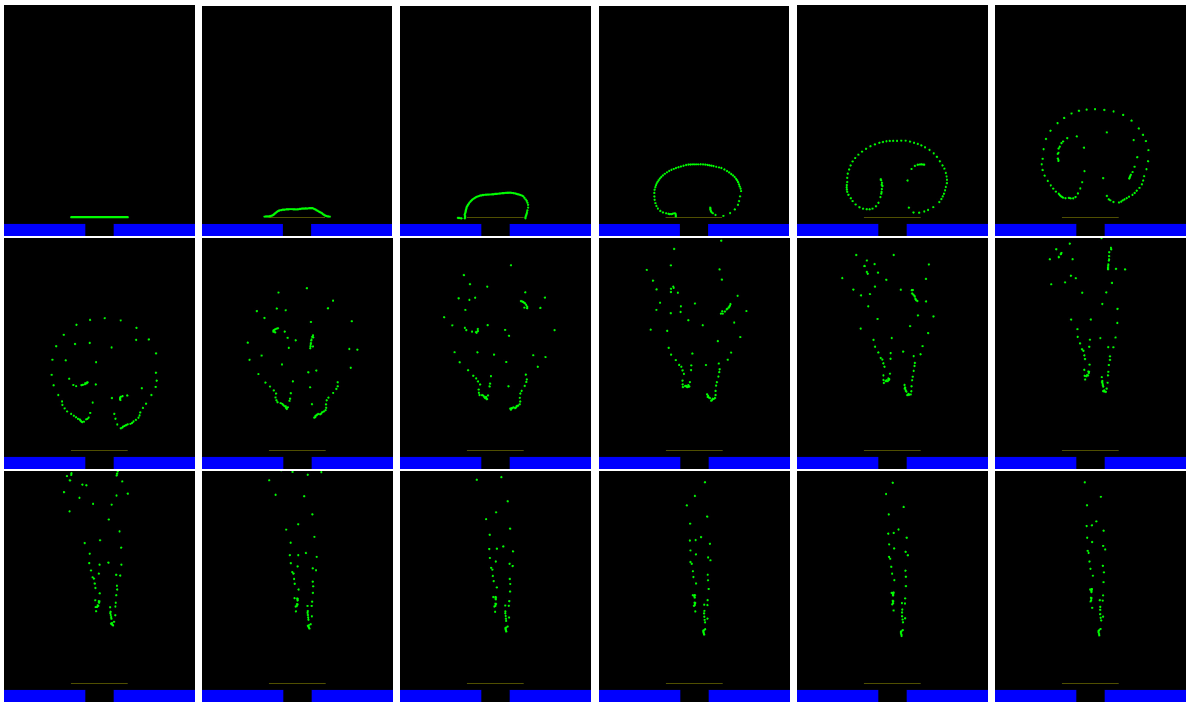

Fig. 14 CFD benchmark study. Particle trajectories as the actuator moves through one cycle, computed from the 250 μm grid experimental data.

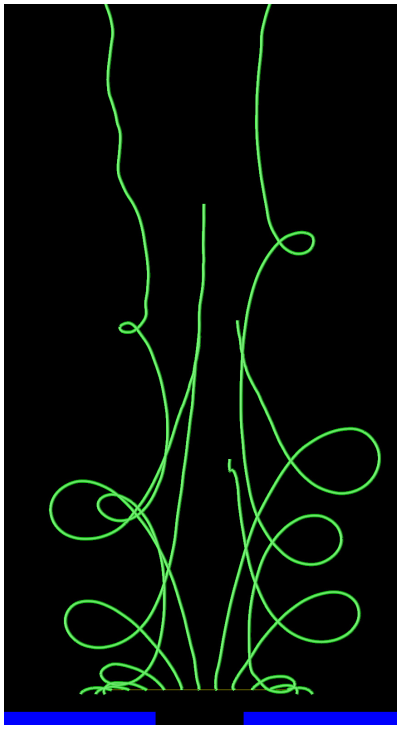

Fig. 13 Pathlines for a set of particles released above the orifice exit at the beginning of the actuator drive cycle, computed from the 250 μm grid experimental data.

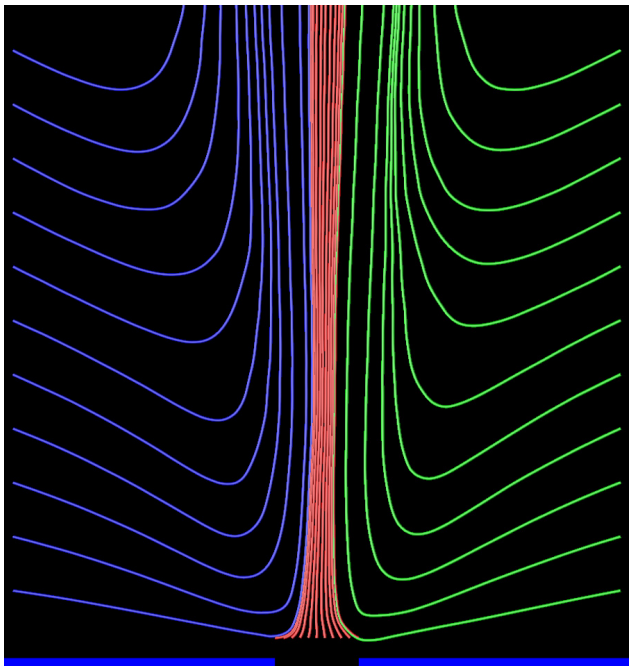

Fig. 15 Mean streamlines for the CFD benchmark actuator, computed from the 250 μm grid experimental data.

in Figure 15. Here the analysis indicates a slight movement of the jet centerline to the right, away from the side of the jet that the diaphragm is located.

Interaction of a Synthetic Jet and a Crossflow

Of key interest in applying the synthetic jet as a flow control actuator is the physics of the interaction of a synthetic jet with a crossflow. To gain some insight

into this interaction, the flowfield caused by the interaction of a synthetic jet and a turbulent boundary layer was examined. By utilizing stereo particle image velocimetry (SPIV), the three components of the velocity field above the actuator were be measured. A single synthetic jet of the type utilized by Chen[18] and a flat plate, zero pressure gradient, turbulent boundary layer were used in this research effort. The actuator was a twin diaphragm, slotted synthetic jet with a slot width of 0.508 mm and a slot length of 35.56 mm. Without the presence of a crossflow, the actuator produced a RMS velocity of 16.5 m/s with a peak velocity of 39 m/s at an operating frequency of 500 Hz.

This research effort was conducted in the NASA Langley 15-inch Low Speed Wind Tunnel of the Flow Physics and Control Branch. This tunnel is a closed-return atmospheric facility dedicated to basic flow physics research efforts. The tunnel has a maximum speed of 115 ft/sec. During this research effort, the tunnel was equipped with a flat plate model that acts a splitter plate. The plate features an elliptical leading edge and immediately downstream of the transition from the leading edge to the flat plate, there is a grit strip to trip the boundary layer of the plate. The ceiling of this tunnel is adjustable at several locations down the length of the tunnel. These supports were adjusted to create a zero pressure gradient over the plate starting from a station 20 inches from the leading edge to a station 50 inches from the leading edge. Flow visualization conducted in this tunnel suggests that the flow is two-dimensional in the zero pressure gradient region of the plate, with the exception of the region close to the wall.[19]

The plate was utilized in this research effort as a false floor. Several synthetic jet actuators were fabricated in plug-like modules that were installed into the bottom of the plate so that the upper surface of the actuator plug is flush with the plate. The installed actuator and the flat plate can be seen in Figure 16. The flat plate was instrumented with a number of pressure taps along the centerline of the tunnel, upstream and downstream of the actuator. These taps were connected via short lengths of flexible tubing to a pressure scanner adjacent to the actuator in a cavity within the plate.

The velocity measurements presented here were carried out with a stereo particle image velocimetry (PIV) system. The timing control, image acquisition, data management and post-processing of the PIV data was handled by a commercially available system. The light source utilized was a pulsed, frequency-doubled 300 mJ Nd:YAG laser operating at 10 Hz. The flow within the tunnel was seeded with atomized mineral oil. The particles have a typical size of 5-10 microns and are injected into the flow in the tunnel settling chamber.[19] Standard sheet-forming optics were utilized and the cameras were positioned on the same side of the tunnel.

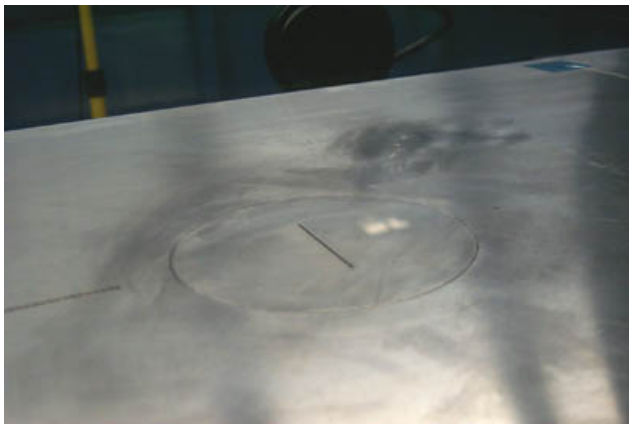

Fig. 16 Synthetic jet actuator installed in the false floor. Slot orientation shown is perpendicular to the freestream

The image acquisition and lasers were synchronized with the drive signal of the synthetic jet so that images could be acquired at a specific phase of the actuator drive signal. The timing delay was varied in order to acquire data at 36 specific phases of the synthetic jet actuator drive signal. These phases were equally spaced in time, recording the velocity field every 10 degrees of phase of the drive signal. For each phase, 100 image pairs were acquired over a period of 10 seconds. These 100 image pairs were processed using a standard cross-correlation technique as implemented in the commercial software package. The entire field of view for the images was 18 mm by 18 mm. Using 50% overlapping of the integration windows, velocity vectors were calculated with a spacing of 200 microns. The 100 measurements of the velocity field recorded for each phase were averaged to yield the phase-average flowfield over the jet at that particular phase. These ensemble averaged velocity fields were then ordered in time allowing the evolution of the jet flow field, and its interaction with the crossflow, to be studied. Figure 17 shows the instantaneous sectional streamlines for one of these phase-averaged ensembles. In this data, the jet is interacting with a crossflow with a freestream Mach number of 0.05. The phase angle here is 80° past the beginning of the ejection phase of the jet. The flow out of the jet during the ejection phase has formed two vortical structures which displace the streamlines away from the wall and "shepherd" this displacement downstream, holding the streamline originally next to the wall between the vortex pair. The boundary layer height in this area is on the order of 12 mm or about twice the displayed height in the figure.

Using the same techniques described in the previous section, the trajectories of individual particles can be followed during the interaction of the jet and the boundary layer. This is shown in Figure 18 for the case of a freestream crossflow Mach number of 0.05. Here

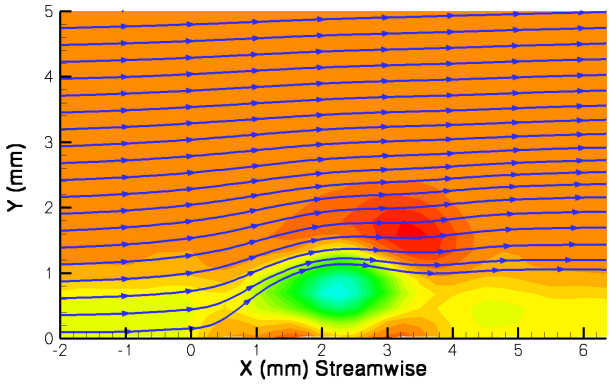

Fig. 17 Instantaneous sectional streamlines for a freestream Mach number of 0.050. Phase angle is 80° after the beginning of the ejection phase.

a set of particles is released five slot widths upstream of the leading edge of the actuator slot (red) and also directly over the slot exit (green). It is clear that the flow from the jet displaces the near wall fluid from upstream, away from the wall for a significant distance downstream of the slot. Figure 18(h) corresponds to the velocity field shown in Figure 17.

This work is an ongoing effort involving not only slot orifices but also circular and elliptical orifices. Also, the effects of different crossflow Mach numbers has been examined. This work will be the subject of a future report.

Conformal Synthetic Jets

One of the challenges that confront a designer that wishes to use synthetic jets is how to integrate the devices into an airfoil. This is particularly challenging when the airfoil is destined for a wind tunnel, where space is at a premium. To support research into using synthetic jets to generate oscillatory blowing,[24] a set of three synthetic jet actuators were designed to be integrated into an fully instrumented, existing wind tunnel model. A generic high lift model consisting of a leading edge slat and a single simple trailing edge flap was chosen for these tests. The three locations chosen for actuation were the shoulder area aft of the leading edge slat, the area directly forward of the flap, on the main body of the wing, and finally on the flap itself. The model was constructed so that each of these areas was installed as an insert into the main body of the model. This allowed an actuator to be designed that can be installed in place of the solid insert, or "plug", that was used for the baseline measurements on the wing. Each of the plugs is bounded by the airfoil curvature on one side and the internal structure of the model on the other sides. Each is relatively shallow in depth, preventing a realistically sized synthetic jet from standing internal to the model and normal to the airfoil surface. To overcome this, the design of a synthetic jet was re-worked so that the actuator diaphragm lies below the surface of the airfoil, parallel to the waterline of the model and the outside, curved airfoil surface of the model forms one of the cavity walls. It is through this external wall, that the jet orifices were formed. This allows the flow from the jet to be directed out of the model at about 30 degrees angle off the local airfoil surface. This design was utilized for each of the actuators plugs. In order to facilitate the testing of a variety of options for the cavity shape and slot geometry, prototype plugs were fabricated by the use of stereo-lithography.

The model is 40 inches in span and 16 inches in chord. A single cavity was created in each actuator and this cavity was excited by multiple piezoelectric actuator disks. If we consider the actuator on the flap as an example, the plug featured a cavity that was 36.3 inches long excited by 18 actuator disks. Each cavity was instrumented with a pressure transducer and the electrical connections for the actuator disks were driven from a common bus bar that ran the length of the plug. This actuator plug was fabricated in sections and the CAD models for one of these sections can be seen in Figure 19. In this figure, the orifice slots and the actuator mounting points can be seen clearly. Figure 20 is a photograph of the model with the trailing-edge and flap actuators installed in the model. For information on the wind tunnel testing of these actuators, the reader is referred to Pack, et. al.[24]

Future Directions

Innovative actuators are a cornerstone component to continued success in flow control. The actuator development effort has provided a focused, centralized location for this work within NASA Langley. The multidisciplinary team approach utilized in this effort has allowed input from multiple disciplines on how various actuator challenges can be addressed and has lead to some unique approaches. The first of these is the application of a commercial off-the-shelf (COTS) device to active flow control. This COTS device is the result of a massive amount of engineering development, optimizing the design to a specific non-flow control application. However, with some modifications, the device also satisfies a number of the requirements for a flow control actuator. The COTS device is currently being applied to an unsteady circulation control wing for general aviation and its use for forebody vortex control is being examined. Extensive pre-test use of CFD modeling was used to refine the integration of this actuator into the wind tunnel model. The use of structural dynamics modeling and optimization made the development of a piezoelectric driven flap-type actuator for use in reducing the acoustic tones generated by a cavity flow possible. Future tool development will be aided by the establishment of a CFD benchmark for a synthetic jet flowfield through a detailed exper-

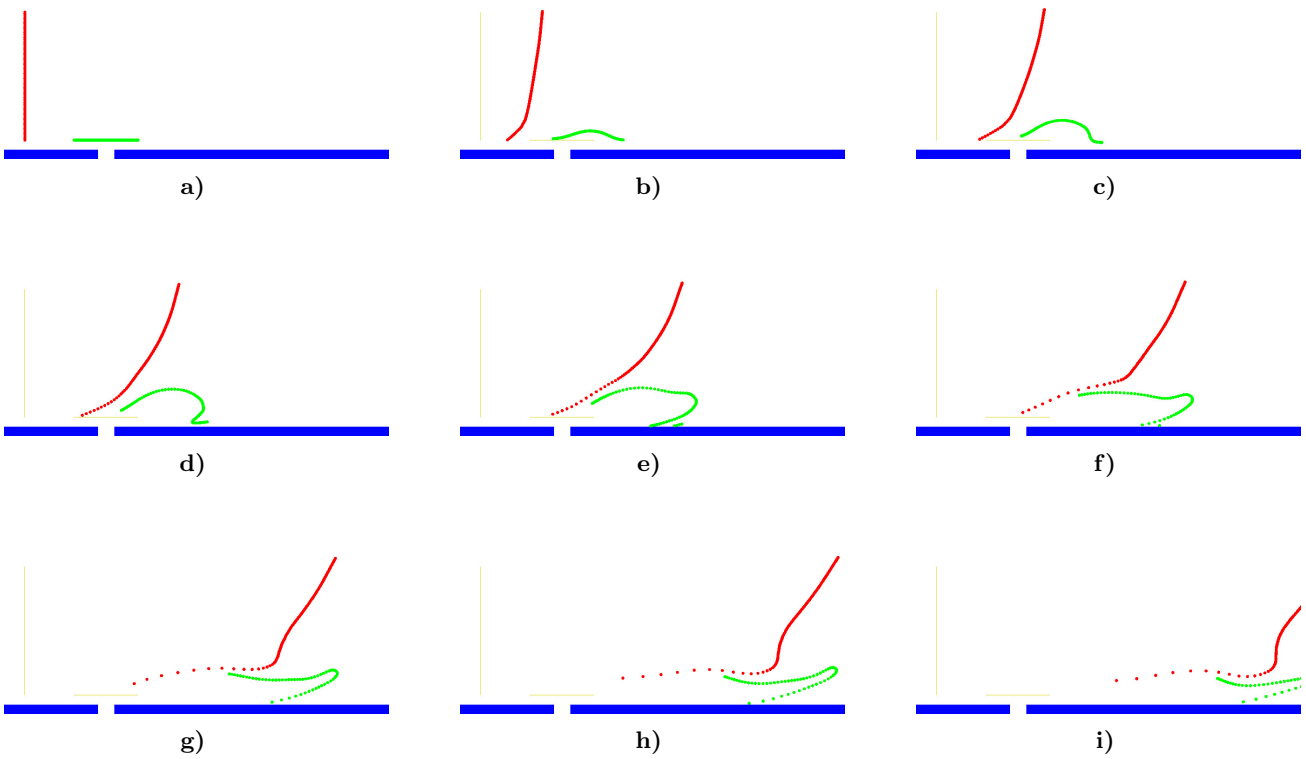

Fig. 18 Interaction of a single synthetic jet with a turbulent boundary layer. Particle trajectories as the actuator moves through first half, exhaust phase, of its cycle, computed from the experimental data. Freestream Mach number is 0.05

imental study and through the detailed study of the interaction between a synthetic jet and a crossflow.

In the future, work will be continuing on these and other fronts. A plasma control actuator[25] is currently being developed that will use plasma dynamics to control aerodynamics flows, even at low speeds. Utilizing the paraelectric effect, a uniform glow discharge actuator can create a local weakly ionized flow over an aerodynamic surface, which can be manipulated through electromagnetic forces. Since the response of such an actuator is highly adjustable, the actuator could be used for such flow control application as on-demand vortex generation, turbulent drag reduction, noise control, or separation control. Also, work is continuing on the development of several high power detonation-based actuator technologies.

References

[1]Prandtl, L., "Motion of Fluids with Very Little Viscosity," *English Translation of "Uber Flussigkeitsbewegug bei sehr kleiner Reibung", Third International Congress of Mathematicians at Heidelberg, 1904, from "Vier Abhandlungen zur Hydrodynamik und Aerodynamik", pp. 1-8, Gottingen, 1927*, NACA TM-452, March 1928.

[2]Gad-el Hak, M., *Flow Control: Passive, Active, and Reactive Flow Control*, Cambridge University Press, Cambridge, United Kingdom, 2000.

[3]Joslin, R. D., "Overview of Laminar Flow Control," NASA TP-1998-208705, Oct. 1998.

[4]Pack, L. G. and Joslin, R. D., "Overview of Active Flow Control at NASA Langley Research Center," *SPIE 5th International Symposium on Smart Structures and Materials, San Diego, California*, SPIE, 1998.

[5]Antcliff, R. R. and McGowan, A. R., "Active Control Technology at NASA Langley Research Center," *Proceedings of the RTO AVT Symposium on "Active Control Technology for Enhanced Perfomance Operational Capabilities of Military Aircraft, Land Vehicles and Sea Vehicles"*, RTO MP-051, Braunschweig, Germany, May 2000, pp. 7–1 – 7–13.

[6]Washburn, A., Althoff Gorton, S., and Anders, A., "A Snapshot of Active Flow Control Research at NASA Langley," AIAA Paper 2002-3155, 2002.

[7]Cattafesta, L., Garg, S., Kegerise, M., and Jones, G., "Experiments on compressible flow-induced cavity oscillations," AIAA Paper 98-2912, 1998.

[8]Kegerise, M. A., *An experimental investigation of flow-induced cavity oscillations*, Ph.D. dissertation, Syracuse University, Syracuse, NY, July 1999.

[9]Williams, D., Fabris, D., Iwanski, K., and Morrow, J., "Closed-loop control in cavities with unsteady bleed forcing," AIAA Paper 2000-0470, 2000.

[10]Cattafesta, L., Garg, S., and Shukla, D., "Development of piezoelectric actuators for active flow control," *AIAA Journal*, Vol. 39, No. 8, 2001, pp. 1562–1568.

[11]Kergerise, M., Cattafesta, L., and Ha, C., "Adaptive Identification and Control of Flow-Induced Cavity Oscillations," AIAA Paper 2002-3158, 2002.

[12]Cattafesta, L., Shukla, D., Garg, S., and Ross, J., "Development of an adaptive weapons-bay suppression system," AIAA Paper 99-1901, 1999.

[13]Englar, R. J., "Circulation Control Pneumatic Aerodynamics: Blown Force and Moment Augmentation and Modification; Past, Present and Future," AIAA Paper 2000-2541, 2000.

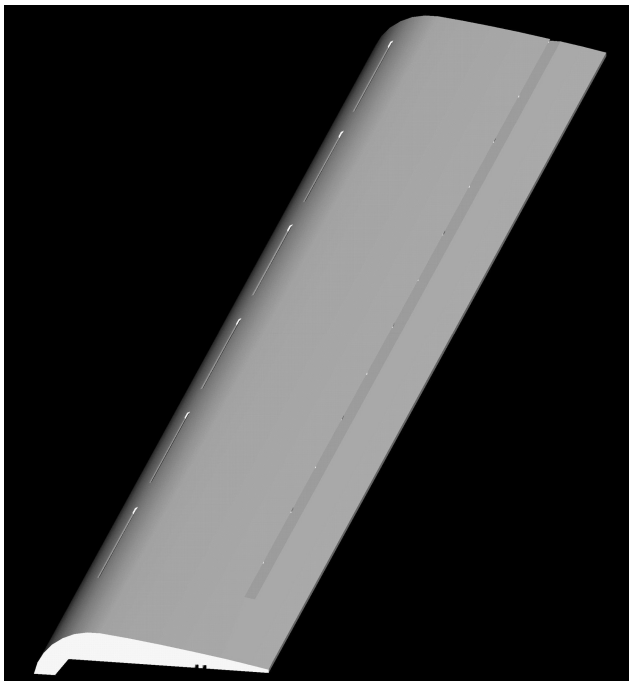

a) Top View

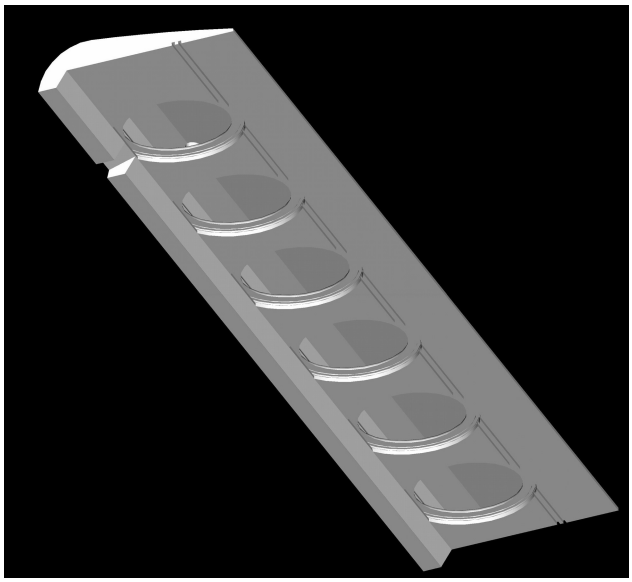

b) Bottom View

Fig. 19 CAD model of the Flap Actuator. Slots are seen in the top view and the actuator mounting points and the electrical connection mountings are seen in the bottom view.

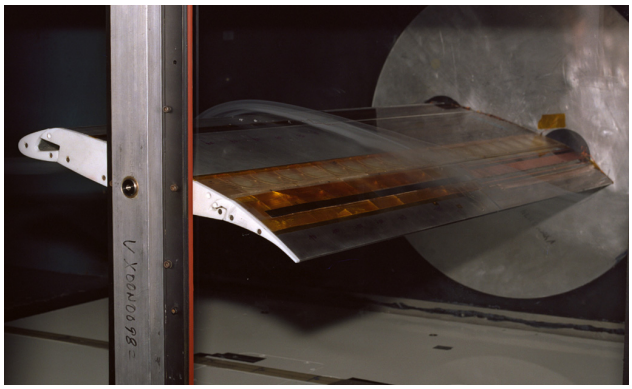

Fig. 20 High Lift model with the trailing edge and flap actuator installed.

[14]Jones, G., Washburn, A., Jenkins, L., and Viken, S., "An Active Flow Circulation Controlled Flap Concept for General Aviation Aircraft Applications," AIAA Paper 2002-3157, 2002.

[15]Smith, B. L. and Glezer, A., "The Formation and Evolution of Synthetic Jets," *Physics of Fluids*, Vol. 10, No. 9, 1998, pp. 2281–2297.

[16]Amitay, M., Smith, B. L., and Glezer, A., "Aerodynamic Flow Control Using Synthetic Jet Technology," AIAA Paper 98-0208, 1998.

[17]Amitay, M., Kibens, V., Parekh, D., and Glezer, A., "The Dynamics of Flow Reattachment over a thick Airfoil Controlled by Synthetic Jet Actuators," AIAA Paper 99-1001, 1999.

[18]Chen, F. J., Yao, C., Beeler, G. B., Bryant, R. G., and Fox, R. L., "Development of Synthetic Jet Actuators for Active Flow Control at NASA Langley," AIAA Paper 2000-2405, 2000.

[19]Jenkins, L., Althoff Gorton, S., and Anders, A., "Flow Control Device Evaluation for an Internal Flow with an Adverse Pressure Gradient," AIAA Paper 2002-0266, 2002.

[20]Gallas, Q., Mathew, J., Kaysap, A., Holman, R., Nishida, T., Carrol, B., Sheplak, M., and Cattafesta, L., "Lumped Element Modeling of Piezoelectric-Driven Synthetic Jet Actuators," AIAA Paper 2002-0125, 2002.

[21]Nichols, C. E., "Preparation of Polystrene Microspheres for Laser Velocimetry in Wind Tunnels," NASA TM-89163, June 1987.

[22]Dring, R. P. and Suo, M., "Particle Trajectories in Swirling Flows," *Journal of Energy*, Vol. 2, No. 4, July-August 1978.

[23]OpenDX, *OpenDX Visualization Software Package, Version 4.2.0*, http://www.opendx.org, 2002.

[24]Pack, L., Schaeffler, N. W., Yao, C., and Seifert, A., "Active Control of Flow Separation from the Slat Shoulder of a Supercritical Airfoil," AIAA Paper 2002-3156, 2002.

[25]Wilkinson, S., "Investigation of the Effect of an Oscillating Surface Plasma on Turbulent Skin Friction," AIAA Paper 2002-3160, 2002.